Title

Mutations in the gene PRRT2 cause paroxysmal kinesigenic dyskinesia with infantile convulsions.

Journal

Cell reports, 1(1)

ISSN

2211-1247

Authors

Lee, Hsien-Yang
Huang, Yong
Bruneau, Nadine
et al.

Publication Date

2012

DOI

10.1016/j.celrep.2011.11.001

Peer reviewed

Cell Reports
Report

Mutations in the Gene *PRRT2* Cause Paroxysmal Kinesigenic Dyskinesia with Infantile Convulsions

Hsien-Yang Lee,[1] Yong Huang,[1,2] Nadine Bruneau,[3] Patrice Roll,[4] Elisha D.O. Roberson,[5] Mark Hermann,[1] Emily Quinn,[1,2] James Maas,[1] Robert Edwards,[1] Tetsuo Ashizawa,[6] Betul Baykan,[7] Kailash Bhatia,[8] Susan Bressman,[9] Michiko K. Bruno,[1,10] Ewout R. Brunt,[11] Roberto Caraballo,[12] Bernard Echenne,[13] Natalio Fejerman,[12] Steve Frucht,[14] Christina A. Gurnett,[15] Edouard Hirsch,[16] Henry Houlden,[8] Joseph Jankovic,[17] Wei-Ling Lee,[18] David R. Lynch,[19] Shehla Mohammed,[20] Ulrich Müller,[21] Mark P. Nespeca,[22] David Renner,[23] Jacques Rochette,[24] Gabrielle Rudolf,[16] Shinji Saiki,[25,29] Bing-Wen Soong,[26,27] Kathryn J. Swoboda,[23] Sam Tucker,[19] Nicholas Wood,[8] Michael Hanna,[8,28] Anne M. Bowcock,[5,28] Pierre Szepetowski,[3,28] Ying-Hui Fu,[1,28,*] and Louis J. Ptáček[1,2,28,*]

[1]Department of Neurology, UCSF, San Francisco, CA 94158, USA
[2]Howard Hughes Medical Institute, San Francisco, CA 94158, USA
[3]Institut de Neurobiologie de la Méditerranée, INMED. Inserm U901. Université de la Méditerranée, 13273 Marseille, Cedex 9, France
[4]INSERM UMR_S910, Université de la Méditerranée, 13385 Marseille, Cedex 05, France
[5]Division of Human Genetics, Department of Genetics, Washington University School of Medicine, Saint Louis, MO 63110, USA
[6]Department of Neurology, University of Florida, Gainesville, FL 32611, USA
[7]Department of Neurology, Istanbul Faculty of Medicine, Istanbul University, Millet Cad 34390, Istanbul, Turkey
[8]Institute of Neurology, University College London, WC1N 3BG London, UK
[9]Department of Neurology, Beth Israel Medical Center, New York, NY 10003, USA
[10]Department of Neurology, The Queen's Medical Center, Honolulu, HI 96813, USA
[11]Department of Neurology, University Medical Centre Groningen, University of Groningen, Groningen, 9713 GZ, The Netherlands
[12]Department of Neurology, Juan P. Garrahan Pediatric Hospital, Combate de los Pozos 1881. CP 1245 Buenos Aires, Argentina
[13]Service de Neuropédiatrie, Hôpital Gui de Chauliac, 34295 Montpellier, France
[14]Movement Disorders Center, Mount Sinai Medical Center, New York, NY 10029, USA
[15]Department of Neurology, Washington University School of Medicine, St. Louis, MO 63110, USA
[16]Service de Neurologie. Hôpitaux Universitaires de Strasbourg, 67091 Strasbourg, France
[17]Parkinson's Disease Center and Movement Disorders Clinic, Department of Neurology, Baylor College of Medicine, Houston, TX 77030, USA
[18]National Neuroscience Institute, 308433 Singapore, Singapore
[19]Division of Neurology, Children's Hospital of Philadelphia, Philadelphia, PA 19104, USA
[20]Clinical Genetics, Guy's Hospital, SE1 9RT London, UK
[21]Institut für Humangenetik, Justus-Liebig-Universität, Giessen, Germany, D-35392
[22]Pediatric Neurology Division, Rady Children's Hospital San Diego, UCSD Department of Neuroscience, San Diego, CA 92123, USA
[23]Department of Neurology, University of Utah, Salt Lake City, UT 84132, USA
[24]Service de Génétique-INSERM UMR 925, Université de Picardie Jules Verne, Amiens 80036, France
[25]Department of Neurology, Kanazawa Medical University, Ishikawa 920-0293, Japan
[26]Department of Neurology, National Yang-Ming University School of Medicine, Taipei 11221, Taiwan
[27]Department Neurology, The Neurological Institute, Taipei Veterans General Hospital, Taipei 11221, Taiwan
[28]Senior Investigator, International Paroxysmal Kinesigenic Dyskinesia/Infantile Convulsions Collaborative Working Group
[29]Present address: Department of Neurology, Juntendo University School of Medicine, Tokyo 113-8421, Japan
*Correspondence: ying-hui.fu@ucsf.edu (Y.-H.F.), ljp@ucsf.edu (L.J.P.)
DOI 10.1016/j.celrep.2011.11.001

SUMMARY

Paroxysmal kinesigenic dyskinesia with infantile convulsions (PKD/IC) is an episodic movement disorder with autosomal-dominant inheritance and high penetrance, but the causative genetic mutation is unknown. We have now identified four truncating mutations involving the gene *PRRT2* in the vast majority (24/25) of well-characterized families with PKD/IC. PRRT2 truncating mutations were also detected in 28 of 78 additional families. *PRRT2* encodes a proline-rich transmembrane protein of unknown function that has been reported to interact with the t-SNARE, SNAP25. PRRT2 localizes to axons but not to dendritic processes in primary neuronal culture, and mutants associated with PKD/IC lead to dramatically reduced PRRT2 levels, leading ultimately to neuronal hyperexcitability that manifests in vivo as PKD/IC.

INTRODUCTION

The paroxysmal dyskinesias (PD) are a heterogeneous group of episodic movement disorders that can be separated on the basis

of factors that precede or precipitate attacks, the nature and durations of attacks, and etiology (Bhatia, 2011; Blakeley and Jankovic, 2002). Individuals are typically completely normal between attacks. Attacks of PD and epileptic seizures share several characteristics. The syndrome of paroxysmal kinesigenic dyskinesia with infantile convulsions (PKD/IC, formerly reported as ICCA syndrome; MIM 602066) typically presents in the first year of life with benign, afebrile infantile convulsions that spontaneously resolve, usually by 2 years of age. In young childhood, these individuals begin having PKD; i.e., frequent but brief movements precipitated by sudden movements or change in velocity of movement (e.g., sitting to standing, standing to walking, walking to running). Patients may experience dozens to hundreds of PKD attacks per day. They typically last less than 5 or 10 s but occasionally may be longer. Interestingly, investigators studying families with autosomal-dominant infantile convulsions had recognized that these individuals also developed paroxysmal movement disorders (Szepetowski et al., 1997). Separately, investigators studying PKD, upon taking closer family histories, recognized that their families were also segregating alleles for autosomal-dominant infantile convulsions (Swoboda et al., 2000). In typical PKD/IC families, variable presentation is usual and patients present with PKD, IC, or both. Interfamilial variable expressivity also exists. Hence, families with IC but no PKD were reported and the majority were considered allelic variants of PKD/IC (Caraballo et al., 2001). Similarly, many PKD families are recognized in whom there is no mention of IC, perhaps because the seizures had resolved, leading to presentation with an episodic movement disorder. The nature of the infantile convulsions and the paroxysmal dyskinesias has been well described (Bruno et al., 2004; Rochette et al., 2008; Swoboda et al., 2000; Szepetowski et al., 1997). The gene associated with PKD/IC has been mapped to chromosome 16 by many groups, and extensive efforts to identify the gene have been ongoing (Bennett et al., 2000; Callenbach et al., 2005; Caraballo et al., 2001; Du et al., 2008; Kikuchi et al., 2007; Lee et al., 1998; Roll et al., 2010; Swoboda et al., 2000; Szepetowski et al., 1997; Tomita et al., 1999; Weber et al., 2004).

After having firmly excluded by sequencing the vast majority of the 180 known or predicted genes in the critical chromosome 16 locus for PKD/IC, we set out to perform whole-genome sequencing from one affected member from each of our six most well-characterized families. Upon examining this sequence, we identified potential mutations in a gene called proline-rich transmembrane protein 2 (*PRRT2,* Entrez Gene no. 112476). We chose to examine this gene in a larger collection of well-characterized families from an international PKD/IC consortium. Our interest in *PRRT2* was strengthened for a number of reasons. We've shown that a mouse model of PNKD exhibits dysregulation of dopamine signaling in the striatum (Lee et al., 2012), and our recent work on the molecular characterization of the protein causing this related disorder showed that it functions in synaptic regulation (Ptáček et al., unpublished data). In addition, PRRT2 was shown in a two-hybrid screen to interact with a synaptic protein, SNAP25 (Stelzl et al., 2005), raising the possibility that PKD/IC might also result from synaptic dysfunction.

RESULTS

Whole-Genome Sequencing

Six samples from six well-defined PKD/IC families (K2916, K3323 [Asian], K3538 [African American], K4874, K4998, and K5471, [Caucasian if not otherwise noted]) were selected for whole-genome sequencing at Complete Genomics, Inc. (CGI). For all of the samples, CGI reported overall > 50× genome coverage, with > 95% of the reference genome called. In the whole genome, the CGI results reported around 500 newly identified nonsynonymous variants in each Caucasian sample, and 729 and 1202 in the Asian and African American samples, respectively.

Of note, we have also analyzed the copy number variations (CNVs) and structural variations (SVs) in the PKD/IC region, in order to see whether there were genomic level insertions, deletions, duplications, translocations, or inversions present in the region (Figure S1 available online). However, and as previously reported (Roll et al., 2010), no major CNVs and SVs that were unique and common to the PKD/IC samples were found.

We summarized all of the coding variants in the extended critical region from D16S403 to D16S3057 (chr16:22,937,651–57, 629,851, NCBI build 37) (Figure S2). Upon initial examination, we did not find a gene with unknown nonsynonymous variants in all six samples. However, there were several genes with previously unidentified nonsynonymous variants in two samples, including *TNRC6A*, *PRRT2*, *GDPD3*, *ZNF267*, and *NLRC5*. In *PRRT2*, the sample from K5471 showed an insertion of a thymine that would lead to a p.E173X mutation. The sample from K3323 had a C-to-T transition causing a p.R240X mutation (Figure 1). A closer look at the original read alignments from WGS evidence files in these genes showed that there were two "no-call" (not having enough reads to be significant) cytosine insertions in *PRRT2* (leading to p.R217Pfs*8) in two additional PKD/IC samples from kindreds K2916 and K4998 (Figure 1 and Figure S3). However, Sanger sequencing of *PRRT2* showed that the C insertion was also present in the remaining two PKD/IC samples from kindreds K3538 and K4874 (Figure 1). The reason for the difficulty in calling the C insertion by CGI might be that the insertion was in a stretch of nine Cs. Because CGI uses a 10+25 short read structure (Drmanac et al., 2010), it had a lower chance to cover the whole stretch of nine or ten Cs in one read. Thus, all six PKD/IC samples were found to have truncating (frameshift or nonsense) mutations in *PRRT2*.

Further Investigation of PRRT2 in Probands from 25 Clinically Well-Characterized PKD/IC Families

Sanger sequencing of the proband from each of the 25 best-characterized families in the International PKD/IC Consortium (including the six discussed above) revealed mutations in 24 of the 25 probands (Figures 1 and 2). Among these, 21 (K821, K2916, K3446, K3534, K3538, K4874, K4962, K4998, K5118, K5212, K5770, K7716, K7717, K7718, K7719, K7720, K7721, K16719, K18113, K19599, K30085, and WashU) had a 1 bp (cytosine, C) insertion between bases 649 and 650 (c.649_650insC). This leads to a frame shift and premature protein termination (p.R217Pfs*8; Figures 1 and 2). Two probands (K3323, K7722) harbored a base-pair change (C to T) that leads to an

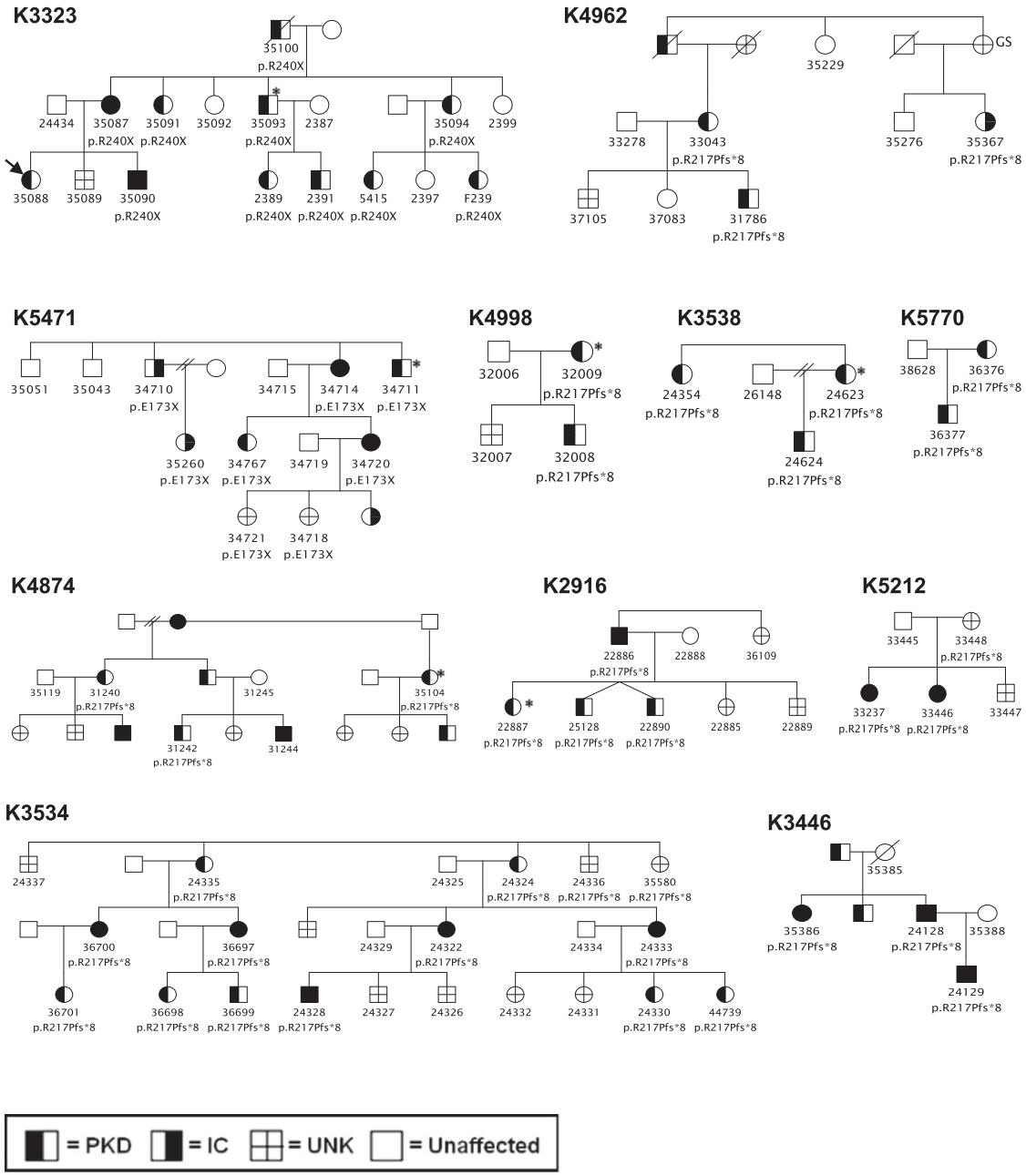

Figure 1. Twenty-Four of Twenty-Five PKD/IC Pedigrees with the Most Secure Phenotypes Carry *PRRT2* Mutations

Eleven of these twenty-four PKD/IC pedigrees are shown. Females are denoted with circles and males with squares. The kindred number is denoted at the upper left corner of each pedigree, and the DNA numbers are noted under individuals for whom they are available. The specific mutation is denoted under each individual, when present. Individuals with a DNA number but no mutation noted have the WT genotype. Affection status for paroxysmal kinesigenic dyskinesia (PKD), infantile convulsions (IC; under the age of 2 years), and GS (generalized seizures; occurring after age 2) are as noted. Samples that were used for WGS are marked with an asterisk (*). One phenocopy was present in K3323 (marked by an arrow).

immediate stop codon at position 240 (p.R240X; Figures 1 and 2). Another proband (K5471) harbored a 1 bp (T) insertion between bases 516 and 517 (c.516_517insT), leading to an immediate stop codon (p.E173X; Figure 1). The remaining one pedigree (K8317, not shown) did not harbor any mutation in *PRRT2*.

Testing of Probands from 78 Less Well-Characterized PKD/IC Families

Additional families were available to us, for whom we have less clinical data, for whom additional family members were not available, or for whom the clinical presentation was somewhat less classic than typical PKD/IC (Bruno et al., 2004). Sanger

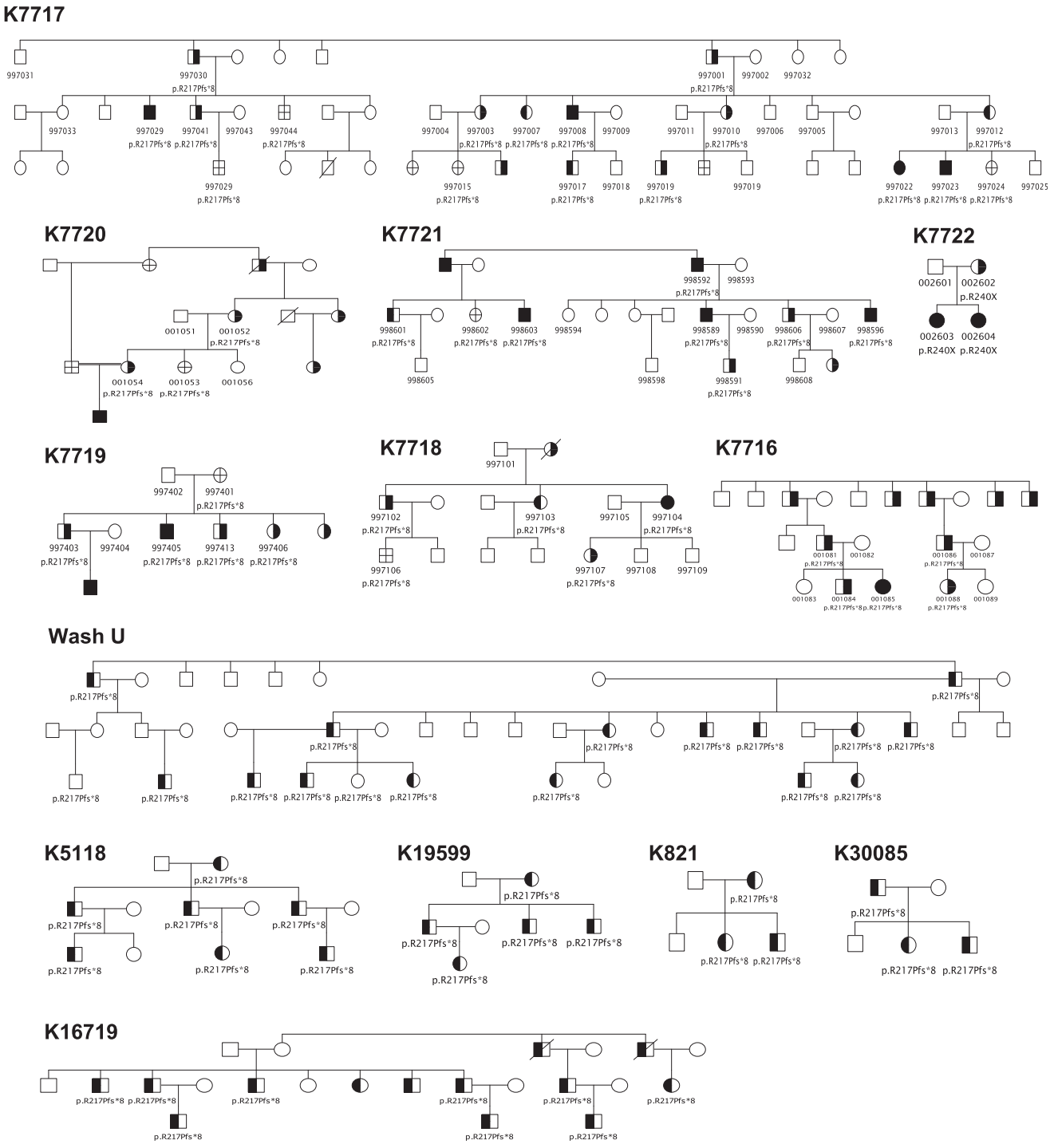

Figure 2. Twenty-Four of Twenty-Five PKD/IC Pedigrees with the Most Secure Phenotypes Carry PRRT2 Mutations

Thirteen of these PKD/IC pedigrees are shown. Symbols are as in Figure 1.

sequencing of these additional 78 probands for whom the clinical diagnosis was considered less secure revealed an additional ten probands (K10615, K50049, K8664, K12206, K50112, K6661, K7920, K9278, K50078, K7253) harboring the p.R217Pfs*8 mutation in familial cases (Figure S4) and 17 with the p.R217Pfs*8 mutation who were isolated cases (data not shown). Finally, one family harbored an unexpected mutation, a 1 bp (T) insertion between bases 980 and 981 (c.980_981insT), leading to a frame shift and stop codon (p.I327Ifs*14) (K3391, Figure S4). Altogether, 28 probands of

the 78 less well-characterized PKD/IC families also had mutations in *PRRT2*.

Examination of Normal Controls for PRRT Newly Identified Alleles

We examined the 1000 Genomes database and the 60 publicly available CGI whole genomes for any of the four alleles that we had identified in PKD/IC patients and did not find them in any of these controls (data not shown). In addition, we sequenced an additional 200 controls and found these alleles in none of them. Thus, these alleles were not present in over 2,500 control chromosomes.

Conservation of PRRT2 across Species

Orthologs of PRRT2 were found in human, gorilla, macaque, mouse, guinea pig, dog, cat, dolphin, and zebrafish, but not in *D. melanogaster* and *C. elegans*. By performing protein sequence alignments, we found that human PRRT2 shared > 90% similarity with other primates (gorilla, macaque), ~80% similarity with most mammals, and ~30% similarity with zebrafish (Figure S5). PRRT2 has two predicted transmembrane domains in its C-terminal sequence. Interestingly, the C-terminal sequences of PRRT2 orthologs were extremely conserved across species. Human PRRT2 showed > 90% similarity of its C-terminal sequence with other mammals and ~60% similarity with zebrafish. The high conservation in the region affected by the mutations suggests an important role of this region of the protein in its biological function.

Testing PRRT2 Variants for Cosegregation with the PKD/IC Phenotype

Next, we tested all available DNA samples in the pedigrees harboring *PRRT2* alleles to test for cosegregation. With the exception of family K3323, in all families for which DNA samples from multiple affected individuals were available, the mutant alleles cosegregated with the phenotype and with the haplotype whenever previously determined (Figures 1, 2, and S4). In K3323 (Figure 1), there was one affected individual who did not carry the disease allele. In light of the fact that so many of our families cosegregated alleles that were not present in a large number of controls, we consider this one individual to be a phenocopy of the PKD/IC phenotype.

Expression of PRRT2 in the Central Nervous System

Human embryonic kidney (HEK) 293T cells transfected with the N-terminal FLAG fusion protein of hPRRT2 were used as positive controls, and untransfected and vector-alone-transfected HEK293T cells were used as negative controls. Western blots of cell extracts were probed with anti-FLAG antibodies and showed a band of ~65 kDa only in the lane from cells transfected with the clone expressing the FLAG-tagged hPRRT2 fusion protein (Figure S6, lane 11). No band was present in lanes with extracts from untransfected cells or those transfected with vector alone (lanes 9, 10). In addition, extracts from eight different mouse tissues were also run on the gel and blotted (lanes 1–8). When the Western blot was probed with an antibody against PRRT2, an identically sized band (~65 kDa) was observed in lanes with extracts from mouse brain and spinal cord (lanes 1 and 8) and in the lane with the extract from HEK293 cells that contained the FLAG-tagged PRRT2 (lane 11). No bands were detected in extracts from peripheral mouse tissues tested at this exposure level (Figure S6). At extended exposures, a faint band of the same size was noted in heart extracts (data not shown). Taken together, these data confirm the specificity of the anti-PRRT2 antibody and the localization of PRRT2 in the central nervous system.

PRRT2 Interacts with SNAP25

The potential interaction between SNAP25 and PRRT2 defined by a two-hybrid screen in a previous report (Stelzl et al., 2005) may be a false positive. Thus, we set out to test whether this interaction is valid. The transmembrane protein prediction software (TMHMM Server and TMpred) indicated that PRRT2 has two putative transmembrane domains at its C terminus. The site of the p.R217Pfs*8 and other mutations relative to the transmembrane domains are diagrammed (Figure 3A). We preformed in vitro coimmunoprecipitation experiments to validate the possible interaction between SNAP25 and PRRT2 in HEK293T cells coexpressing FLAG-tagged SNAP25 and either the WT or the mutant form (p.R217Pfs*8) of HA-tagged PRRT2. After pull-down of FLAG-tagged SNAP25 with FLAG antibody, HA-tagged WT PRRT2 can be detected with anti-HA antibody on Western blot of HEK293T extracts cotransfected with FLAG-SNAP25 and WT HA-PRRT2 (Figure 3B). The reciprocal experiment using an anti-HA antibody to pull down tagged Prrt2 demonstrated that SNAP25 could be detected with anti-FLAG antibody (data not shown). Brain extracts from control mice were then used to pull down Snap25 with anti-Snap25 antibody, and after Western blotting, Prrt2 could be detected with anti-PRRT2 antibodies (Figure 3C). Taken together, these results indicate that PRRT2 interacts with SNAP25 both in vitro and in vivo.

Truncated PRRT2 Failed to Express Normally in Vitro

Surprisingly, we did not detect obvious expression of mutant HA-PRRT2 (R217Pfs*8) in transfected HEK293T cells (Figure 3B), implying that the mutant form of PRRT2 was either unstable or was not expressed at all in this heterologous system and in turn lost its ability to interact with SNAP25. These experiments were then repeated with the three other mutant alleles. Results indicated that all four truncation mutations showed remarkably reduced (R240X and I327Ifs*14) or absent (R217Pfs*8 and E173X) expression when transfected alone (Figure 4, left side). When cotransfected with wild-type (WT) *PRRT2*, PRRT2 protein was present, suggesting that the mutation did not exert a dominant-negative effect on protein levels (Figure 4, right side). This is consistent with the idea that PKD/IC mutations are loss-of-function (haploinsufficiency) mutations, as well as with the single reported case of an individual with possible PKD/IC who harbors a deletion encompassing *PRRT2* (Lipton and Rivkin, 2009).

Cell Localization Studies

We transfected rat hippocampal neuron cultures with either WT or mutant forms (R217Pfs*8) of PRRT2. PRRT2 was present in thin, MAP2-negative processes extending from neuron cell bodies that overlap with synapsin-positive puncta (Figures 5A

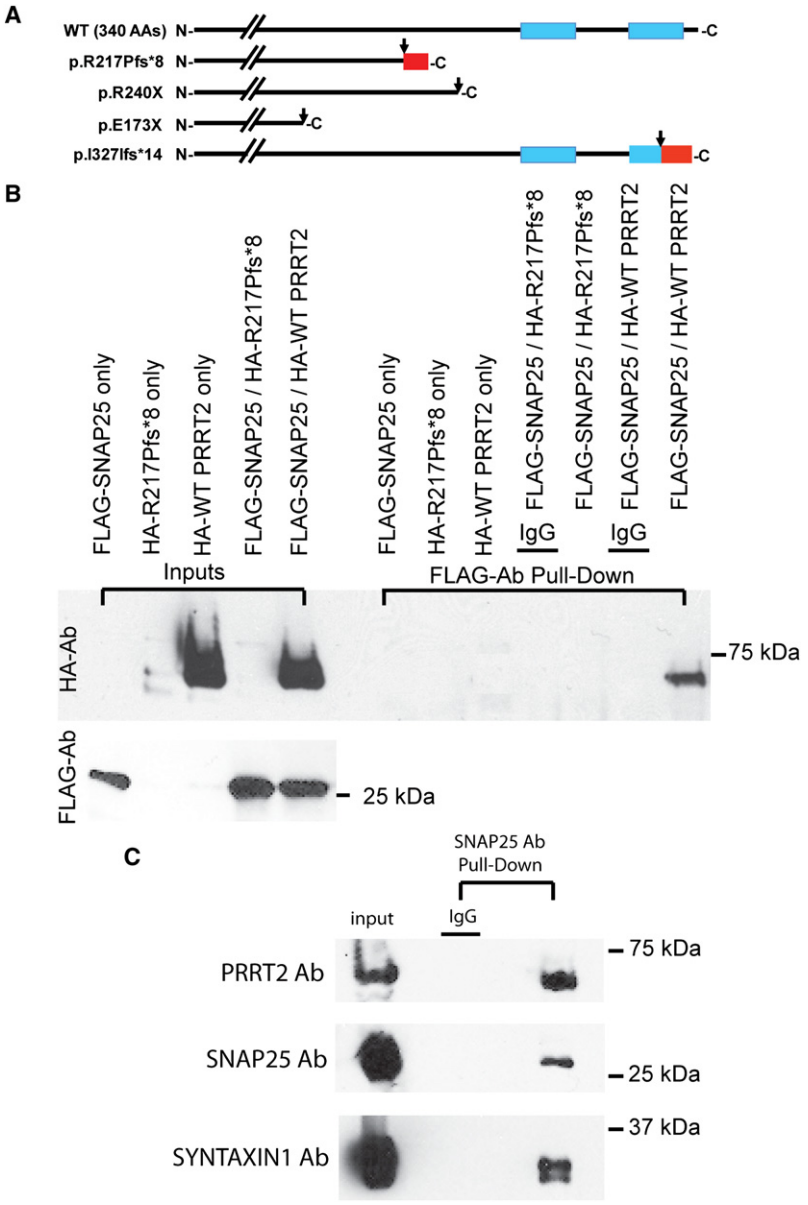

Figure 3. PRRT2 and SNAP25 Interact In Vitro and In Vivo

(A) The comparison of protein structures for WT and truncated mutants of PRRT2. The blue rectangles represent putative C-terminal transmembrane domains of PRRT2. The black arrows represent positions of mutations producing either nonsense or frameshift mutations. Red rectangles represent protein sequences produced by frameshift mutations.

(B) In vitro coimmunoprecipitation was performed in HEK293T cells singly transfected or cotransfected with FLAG-tagged SNAP25 and either HA-tagged WT or mutant forms (p.R217Pfs*8) of PRRT2. After FLAG antibody pull-down, only the cell extract from HEK293T cells cotransfected with FLAG-tagged SNAP25 and HA-tagged WT PRRT2 showed an ~65 kDa band (upper panel, rightmost lane), implying that an interaction exists between SNAP25 and PRRT2 in vitro. Interestingly, no obvious expression was detected in cell extracts transfected with the mutant form of PRRT2 (upper panel, second and fourth lanes from the left).

(C) In vivo coimmunoprecipitation of Snap25 and Prrt2 using whole-brain extracts from a control mouse. After SNAP25 antibody pull-down, a Prrt2 band (~65 kDa) was detected with the use of an anti-PRRT2 antibody. An antibody specific for SYNTAXIN1, a protein interacting with SNAP25, was also used as a positive control.

and 5B), as well as synaptophysin and SV2 puncta (data not shown), indicating that it localized predominantly in axons. Importantly, PRRT2 R217Pfs*8, the most common PRRT2 mutation in PKD/IC patients, led to complete abrogation of PRRT2 expression in cultured neurons (Figure 5C). This result matched our observations in the coimmunoprecipitation experiment described above (Figures 3B and 4).

DISCUSSION

PKD/IC is a fascinating disorder combining an infantile form of epilepsy with a paroxysmal and reflex form of movement disorder. The relationship of PD with epileptic seizures has long been suspected, and genetic studies demonstrated that PKD and IC share common molecular mechanisms (Szepetowski et al., 1997). Despite intensive and multicenter efforts, the disease gene remained unknown until now. PKD/IC and PNKD appear to be genetically homogeneous; most families with clinically "classical" disease have mutations in the recognized genes (Bruno et al., 2007, and data presented here). *PRRT2* mutations that segregated with the disease were found in nearly all (24/25) of our most well-characterized PKD/IC families, including the largest multigenerational ones. Indeed, previous studies predicted a high level of genetic homogeneity (Bennett et al., 2000; Callenbach et al., 2005; Caraballo et al., 2001; Kikuchi et al., 2007; Lee et al., 1998; Roll et al., 2010; Swoboda et al., 2000; Szepetowski et al., 1997; Tomita et al., 1999; Weber et al., 2004). The mutations occur in a highly conserved part of the gene, are not present in controls, and lead to near absence of mutant protein expression in vitro.

Whether the family with negative screening has a *PRRT2* mutation in noncoding sequences or deletion of an entire exon has not been resolved. When other smaller and less well-characterized PKD/IC families and isolated patients were screened, an important proportion of them were also found to have *PRRT2* mutations. In total, 52/103 of all index cases had mutations in *PRRT2*. Obviously some of the "negative" patients are probably misdiagnosed as having PKD/IC. Others might have a disease that is different from, albeit similar to, typical PKD/IC. This topic has been discussed in a previous review of a large collection of PKD patients (Bruno et al., 2004); moreover, nongenetic forms of

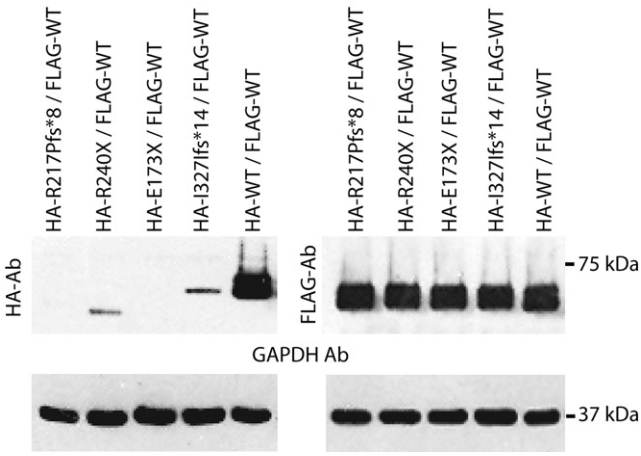

Figure 4. Truncated Mutations of *PRRT2* Lead to Abnormal Protein Expression In Vitro

When HEK293T cells were cotransfected with FLAG-tagged PRRT2 and HA-tagged PRRT2, an ~65 kDa band was present when probed with antibody for the tag on the WT fusion protein, but FLAG-tagged fusion proteins for the truncation mutations showed a significant reduction (R240X and I327Ifs*14) or undetectable expression (R217pfs*8 and E173X). Thus, the mutations led to low or undetectable PRRT2 protein levels that did not affect the WT allele in vitro. GAPDH antibody was used as a sample loading control.

IC and of PKD/IC have been reported (Abe et al., 2000; Camac et al., 1990; Clark et al., 1995; Drake, 1987; Hattori and Yorifuji, 2000; Huang et al., 2005; Mirsattari et al., 1999; Zittel et al., 2011). It is noteworthy that we had previously identified *PRRT2* variants in a small number of families but had not pursued them immediately as one did not cosegregate with the disease in K3323. We now know this is the result of a phenocopy in this family.

The present identification of *PRRT2* as the major gene responsible for the syndrome of PKD/IC represents a crucial entry point to elucidate the pathophysiology of this disorder. An interesting aspect of the disease relates to its natural history. The afebrile seizures typically develop in infancy and resolve by the second year of life. The movement disorder can begin from infancy through adolescence and continues through young adult life. However, in a majority of patients, the movement disorder gets significantly better or completely resolves as patients grow into middle adult life (Bruno et al., 2004). Whether these temporal changes in the expression of the disease are due to developmental differences in the expression of *PRRT2*, epigenetic changes in *PRRT2* with aging, or another cause remains to be studied. In some PKD/IC patients, seizures can also occur in other contexts (febrile convulsions, generalized seizures in adult patients, etc.). It is not clear whether this reflects coincidence of these common disorders with PKD/IC or whether PKD/IC lowers the threshold for other forms of epilepsy.

PKD/IC shares striking clinical and genetic similarity with paroxysmal nonkinesigenic dyskinesia (PNKD). PNKD is a related movement disorder in which individuals experience similar dyskinetic attacks that are typically less frequent, longer lasting, and not initiated by sudden movements (Demirkiran and Jankovic, 1995; Tarsy and Simon, 2006). These patients are not recognized to have a related seizure phenotype but may have an increased risk of migraine in comparison to the general population (L.P., unpublished data) (Bruno et al., 2004; Bruno et al., 2007; Swoboda et al., 2000). In these patients, ingestion of caffeine or alcohol can precipitate attacks, which can last for 1–4 hours (Bruno et al., 2007). Both are highly penetrant, autosomal-dominant disorders that exhibit a spectrum of episodic hyperkinetic movements ranging from choreoathetosis (dance-like and writhing movements) to dytonias (movement of limbs, trunk, or face into a fixed position). Between attacks, patients appear completely normal. The dyskinesias typically become evident in childhood, worsen through adolescence, and often improve as patients grow into middle age (Bruno et al., 2004; Bruno et al., 2007). The threshold for inducing attacks in PKD/IC and PNKD is lowered by stress. The clinical similarities between these two disorders suggest the possibility that they may share some similarities at a molecular and pathophysiological level.

Another phenotype similar to PKD/IC and PNKD has been well studied and may occasionally be associated with epilepsy. Paroxysmal exercise-induced dyskinesia (PED) is a disorder in which individuals experience dyskinesias after prolonged bouts of exercise. All three phenotypes can exhibit clinical dystonia (PNKD as DYT8, PED as DYT9, and PKD/IC as DYT10) (Müller, 2009). The gene associated with a glucose transporter (GLUT1) has recently been shown to be mutated in some families with PED (Schneider et al., 2009; Suls et al., 2008; Weber et al., 2008). Given the similarities among these three disorders, it is interesting to speculate about possible similarities in pathophysiology. Of the three, the most is known about pathophysiology in PNKD, with recent insights about the role of PNKD in synaptic regulation and the effect of mutations in dysregulation of dopaminergic signaling (Lee et al., 2004; Ptáček et al., unpublished data). Here, we present circumstantial evidence suggesting the possibility that PKD/IC may also result from dysfunction of an unexpected protein in synaptic regulation (through an interaction with SNAP25), though much work remains to either prove or disprove this hypothesis. Finally, what role is a glucose transporter playing in a dyskinesia disorder, particularly one that comes on after prolonged exercise (as opposed to coincident with the onset of movement, as in PKD)? One possibility is that an energy-dependent process such as synaptic regulation of neuronal excitability may initially function normally but fail if the energy source is insufficient to keep up with the need under conditions of higher neuronal firing rates.

On the basis of other episodic disorders, it had long been predicted that PKD/IC might be a channelopathy (Ryan and Ptácek, 2010). However, multiple groups have previously ruled out genes from the region known to encode channel-related proteins and other physiologically relevant proteins such as those known to function at the synapse. *PRRT2* is a proline-rich protein that was suggested to interact with synaptosomal-associated protein 25 kDa (SNAP25). SNAP25 is a presynaptic membrane protein involved in the synaptic vesicle membrane docking and fusion pathway (Zhao et al., 1994); it plays a pivotal role in calcium-triggered neuronal exocytosis (Hu et al., 2002; Sørensen et al., 2002). This is consistent with previous studies on PNKD, which is a synaptic protein regulating exocytosis (Ptáček et al., unpublished data) and involved in dopamine signaling

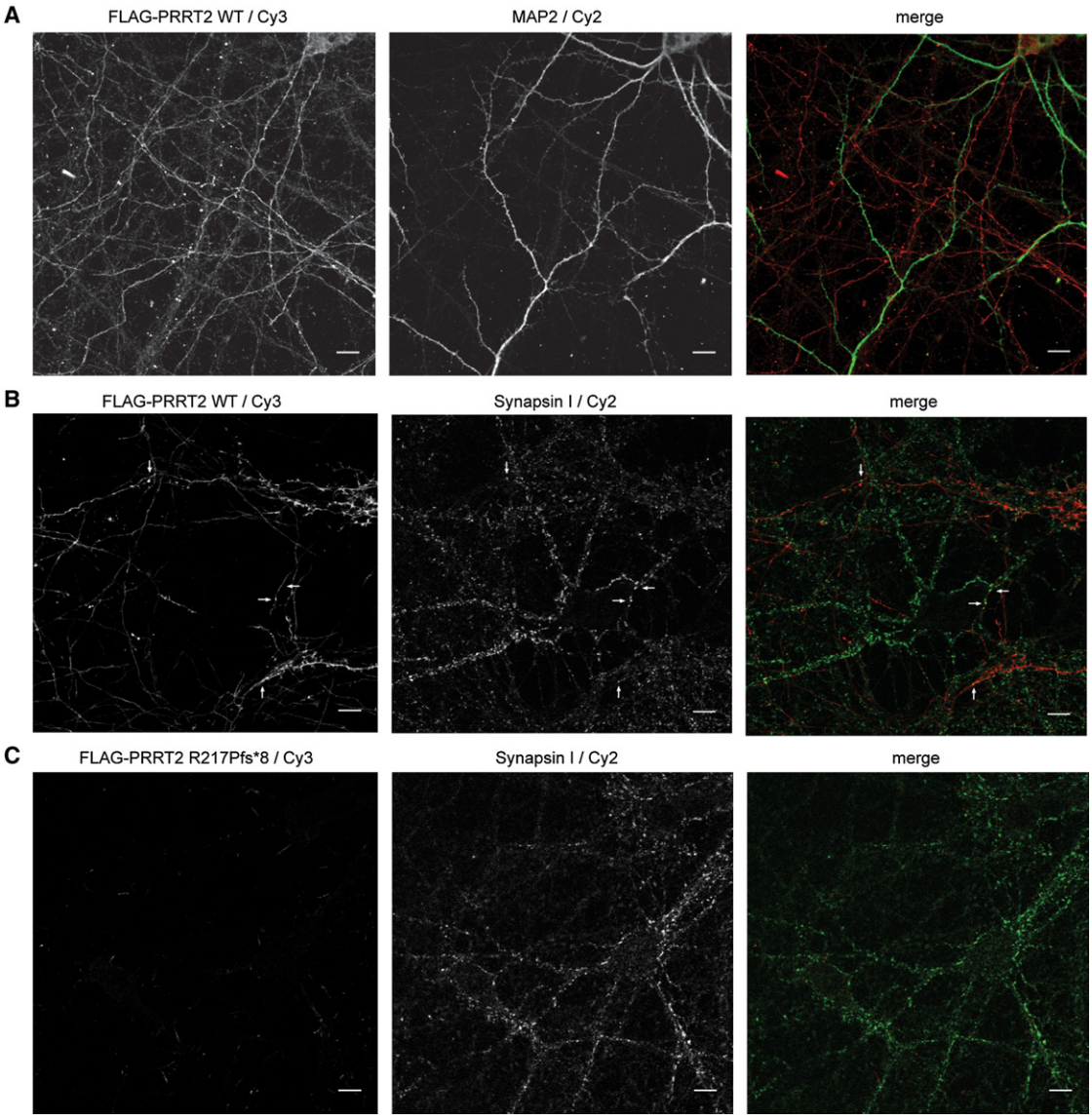

Figure 5. Expression and Localization of PRRT2 in Hippocampal Neurons

(A) Coimmunostaining of WT FLAG-PRRT2 and MAP2 showed distinct localization patterns.

(B) Coimmunostaining for WT FLAG-PRRT2 and synapsin I showed that WT PRRT2 colocalized with synapsin I in neuronal puncta.

(C) After coimmunostaining of the FLAG-PRRT2 R217Pfs*8 mutant with synapsin I, no obvious positive staining of mutant PRRT2 was detected. Red, WT FLAG-PRRT2; green, MAP2 or Synapsin1. Scale bars represent 10 μm.

(Lee et al., 2012). Interestingly, one atypical patient with deletion of a region encompassing *PRRT2* had not only PKD and possibly infantile-onset convulsions, but also DOPA-responsive parkinsonism (Lipton and Rivkin, 2009). If indeed this deletion causes the phenotype in this patient, it argues for a loss-of-function mechanism. This would be consistent with the near absence of protein expression that we saw when expressing the *PRRT2* mutations in HEK293 cells and cultured neurons and with the persistence of protein on Western blots when WT and mutant constructs were coexpressed.

Here, we show that PRRT2 localizes to neurons and that the human mutations lead to near absence of mutant protein in vitro. This latter observation could be due to nonsense-mediated RNA decay. Alternatively, the mRNA and protein may be expressed and translated but degraded very quickly. Such possibilities can be resolved in future work.

Additional studies are now needed to understand how and when the disturbance of synaptic functioning leads to a heterogeneous syndrome with episodic, variable, and age-dependent cortical and subcortical clinical manifestations. Cloning of the causative gene for this complex disorder has been a Herculean task that has taken nearly 15 years, and now the recognition of the causative role of *PRRT2* enables many new lines of experiments that will accelerate the pace of discovery into pathways

relevant to the hyperexcitability giving rise to dyskinesias in these patients.

EXPERIMENTAL PROCEDURES

Patient and Family Data Collection

PKD/IC patient and family data were collected as previously described (Bennett et al., 2000; Bruno et al., 2004; Caraballo et al., 2001; Lee et al., 2004; Swoboda et al., 2000; Szepetowski et al., 1997; Thiriaux et al., 2002). The country of origin and ancestry of the enrolled research subjects is shown in Table S1.

Whole-Genome and Whole-Exome Sequencing

Whole-genome sequencing (WGS) was carried out at Completegenomics (CGI). Fifteen micrograms of genomic DNA was submitted for each sample. Front-end data analysis, including sequence mapping and assembly and variant calling, was included in the CGI service. The resulting data from CGI included variant calls (including the original variant calls, their functional annotations, and summary by gene), CNV, and SV calls, as well as the alignment and coverage files. WGS samples of other diseases studied by our group and samples from the CGI public genomes, 70 genomes in total, were used as controls in this study.

For PKD/IC, we focused on the genomic region between D16S403 and D16S3057 (chr16:22,937,651–57,629,851; NCBI build 37), which covered all of the critical regions previously reported in PKD/IC linkage analyses. We retrieved all of the variants in the genomic region from the WGS results of the PKD/IC samples and reorganized them by their host genes along the chromosome. Variants that were also present in the control genomes were filtered out. We were particularly interested in variants that were not present in dbSNP (build 131), control WGS genomes, or the 1000 Genomes data. Genes with newly identified nonsynonymous variants in multiple samples were given high priority for further examination. We have also examined the additional region from D16S3057 to D16S503, based on a very recent report (Ono et al., 2011) (data not shown).

With the WGS data, we have also examined whether there were CNVs and SVs common among the PKD/IC samples and not in the control genomes (Figure S7). CGI estimated the copy number on the basis of the normalized counts of reads (read depth) aligned to genomic regions. The window width for calculating the CNV is 2 kb. We visualized and compared the CNV results from CGI with the Integrated Genome Viewer (Robinson et al., 2011). We converted the junction data to SVs with cgatools and then visualized and compared them with custom scripts and Circos.

Three members of the Wash U family (Figure 2; Table S2) were subjected to exome sequencing with Nimblegen SeqCap EZ Exome capture and either Solexa GAIIx 76-cycle paired-end sequencing or 101-cycle HiSeq. Sequence data were aligned to hg19 with the Burroghs-Wheeler Aligner (BWA v0.5.7), optical duplicates were marked with Picard (v1.29), and variants were extracted with SAMtools (v0.1.8). Data were filtered for common variants with the use of dbSNP130, 1000 Genomes, and information from eight HapMap individuals as described elsewhere (Harbour et al., 2010).

PCR and Sanger Sequencing of DNA Samples

PRRT2 was screened for mutations via Sanger sequencing of genomic DNA. Coding regions in DNA of the PKD/IC probands were selected for initial PCR sequencing. Twenty-five microliters of PCR reactions were carried out per 100 ng of genomic DNA and 10 pmol of both forward and reverse primers. Primers were designed outside of splice sites with the intent that intronic sequencing of at least 50 bp would flank each exon border. PCR procedures that led to successful product amplification were as follows: 98°C, 30 s (98°C, 10 s; 60°C, 30 s; 72°C, 40 s) × 35, 72°C, 10 min, and 4°C hold. PCR product purification was performed with the use of the PCR_{96} Cleanup Plate (Millipore), followed by sequencing. Exon 2 and exon 4 of PRRT2 are too large to be amplified by a single primer pair, so multiple overlapping primer pairs were used. Exon 2 was broken into three fragments (2A–2C), while exon 4 was broken into two (4A and 4B). All primer sequences and conditions for the four exons are included in Table S3.

Analysis of PRRT2 Sequence Conservation Across Species

In the search for homologous genes, the orthologous sequences of PRRT2 across different species were identified from publicly available online databases (Ensembl, UCSC Genome Bioinformatics, and NCBI). The ClustalW2 program was used for multiple sequence alignment of PRRT2 orthologs. For PRRT2 ortholog C-terminal sequences comparison, the transmembrane protein prediction programs (TMHMM and TMpred) were used for prediction of individual PRRT2 C-terminal sequences that potentially form the transmembrane domains, then these C-terminal sequences were aligned and compared by the ClustalW2 program.

Cloning of WT and Mutant PRRT2

The *PRRT2* plasmid clone (clone ID 5729288) from Open Biosystems (Thermo Scientific) was used as the backbone for cloning WT *PRRT2*. The primer sets containing EcoRI and BamHI sites at 5′ and 3′ ends were used to clone WT *PRRT2*. The sequences of cloning primers are listed below: primer-F, 5′-ACT GACGAATTCCATGGCAGCCAGCAGCTCT-3′ (with EcoRI site); and primer-R, 5′-ACTGACGGATCCTCACTTATACACGCCTAA-3′ (with BamHI site). The WT *hPRRT2* was amplified via PCR from the backbone plasmid and gel-purified with the QIAquick Gel Extraction Kit (QIAGEN), followed by digestion with EcoRI and BamHI and then purification by the QIAquick PCR Purification Kit (QIAGEN), then it was cloned into the N-terminal p3XFLAG-CMV-10 expression vector (Sigma-Aldrich) with the use of the T4 DNA ligase (Promega). For cloning of *PRRT2* c.649_650insC (PRRT2 R217Pfs*8), site-directed mutagenesis was performed with the QuikchangeII Site-Directed Mutagenesis Kit (Agilent Technologies), and the primers for mutagenesis were as follows: mutF1, 5′-GGCCCCCCCCCCGAGTGCTGCAG-3′; mutR1, 5′- CTGCAGCAC TCGGGGGGGGGGCC-3′; for *PRRT2* c.649_650insC. For transfection of WT and mutant *PRRT* into primary neuronal culture, the N-terminal FLAG-tagged WT and mutant *PRRT* in p3XFLAG-CMV-10 expression vector were used as templates and recloned into the pCAGGS/ES expression vector. The primers for subcloning contained NheI and EcoRV sites at 5′ and 3′ ends, and their sequences are as follows: FLAG-F, 5′-ATCGATGCTAGCATGGACTACAAA GACCATGACGGTGATTAT-3′ (with NheI site); FLAG-R, 5′-ATCGATGATA TCTCACTTATACACGCCTAAGTTGATGAC-3′ (with EcoRV site).

Western Blotting

Male C57/B6 mice were sacrificed, and different tissues, including brain, spinal cord, spleen, kidney, heart, liver, skeletal muscle, and testes, were dissected and homogenized in RIPA buffer (10 mM Tris-HCl [pH 7.2], 150 mM NaCl, 5 mM EDTA, 1% Triton X-100, 1% SDS, 1% Deoxycholate) with protease inhibitor (Roche) and Phosphatase Inhibitor Cocktails (Sigma). For positive control of PRRT2 antibody, HEK293T cells were transfected with plasmid DNA (p3XFLAG-PPRRT2 WT construct and p3XFLAG-CMV-10 vector alone) with the use of the FuGene HD transfection reagent (Roche Diagnostics GmbH), grown, and harvested 36 hr later after transfection. HEK293T cells were then homogenized in 1 ml of RIPA buffer with protease and phosphatase inhibitors. Mouse tissue and HEK293T homogenates were resolved on 10% polyacrylamide gels and electroblotted to nitrocellulose membrane with 50 mM Tris-HCl buffer (pH 8.4). The blot was incubated with a rabbit anti-PRRT2 antibody (1:1000, Sigma) overnight at 4°C, then incubated with goat anti-rabbit IgG-HRP (1:5000, Santa Cruz Biotechnology) at room temperature for 1 hr, then detected with Immobilon Western Chemiluminescent HRP substrate (Millipore). Blots were stripped and reprobed with a mouse anti-FLAG antibody (1:5000; Sigma), followed by the procedure described above.

Coimmunoprecipitation Experiment for Testing the Interaction between SNAP25 and PRRT2

The *SNAP* plasmid clone (clone ID 3867544) from Open Biosystems was used as the backbone for cloning *SNAP25*. The primer sets containing EcoRI and BamHI sites at 5′ and 3′ ends were used to clone *SNAP25*. The sequences of cloning primers are as follows: primer-F, 5′-ACTGACGAATTCATGGCC GAAGACGCAGACATGCGCAATG-3′ (with EcoRI site); primer-R, 5′-ACT GACGGATCCTTAACCACTTCCCAGCATCTTTGTTGC-3′ (with BamHI site). *SNAP25* was then cloned into the N-terminal p3XFLAG-CMV-10 expression vector by the procedure described above. The *PRRT2* plasmid clone from Open Biosystems was used as the backbone for cloning N-terminal HA-tagged

PRRT2. The primer sets containing NcoI and EcoRI sites at 5′ and 3′ ends were used to clone WT HA-tagged *PRRT2,* and the sequences of cloning primers are as follows: primer-F, 5′-CATGCCATGGCATGCATGGCAGCCAGCAGCTCT GAGATCTCTGAG-3′ (with NcoI site); primer-R, 5′-CCGGAATTCCCGTCACT TATACACGCCTAAGTTGA-3′ (with EcoRI site). *PRRT2* was then cloned into the pEF1-αHA vector (Clontech Laboratories). The mutant form of N-terminal HA-tagged *PRRT2* (c.649_650insC, R217Pfs*8) was made from the WT HA-*PRRT2* clone by the site-directed mutagenesis described above. HEK293T cells were grown in Dulbecco's modified Eagle's medium (DMEM) supplemented with penicillin, streptomycin, and 10% fetal bovine serum (Invitrogen) and maintained at 37°C with 5% CO_2. After 1 day, the cells were split into 10 cm dishes. In parallel, HEK293T cells grown to 80%–90% confluence were transfected with DNA (p3XFLAG-CMV-10 SNAP25, pEF1-αHA-*PRRT2*-WT fusion construct, pEF1-αHA-*PRRT2*-c.649_650insC fusion construct, and SNAP25 cotransfected with the WT or mutant form of the pEF1-αHA-*PRRT2* fusion construct) with the use of FuGene HD transfection reagent. Twenty-four to thirty-six hours after transfection, cells were harvested and homogenized in RIPA buffer containing protease and phosphatase inhibitors. The HEK293T extracts were then applied in the coimmunoprecipitation experiments performed with the use of an immunoprecipitation kit (Roche) in accordance with the manufacturer's instructions. During the coimmunoprecipitation process, the mouse anti-FLAG M2 monoclonal antibody (1:1000, Sigma) was used to pull down the FLAG-tagged SNAP25, and rabbit anti-HA tag antibody (1:1000, Abcam) was subsequently used for detecting HA-PRRT2 fusion proteins in HEK293T cell extracts. The normal mouse IgG (1:1000, Santa Cruz Biotechnology) was used as a control of antibody pull-down. For in vivo coimmunoprecipitation experiments, whole brains from male C57/B6 mice were homogenized in RIPA buffer with protease inhibitor and phosphatase inhibitor cocktails (3 mL/brain). Mouse whole-brain extracts were used in coimmunoprecipitation experiments with the use of a kit according to the manufacturer's instructions. During the process, rabbit anti-SNAP25 antibody (1:20, Cell Signaling Technology) was used to pull down Prrt2, and rabbit anti-PRRT2 antibody (1:1000) was subsequently used for detecting Prrt2 proteins in mouse whole-brain extracts. Rabbit IgG (1:1000, Santa Cruz Biotechnology) was used as a control for antibody pull-down. The mouse anti-Syntaxin1 antibody (1:1000, Synaptic Systems GmbH) was used for detecting Syntaxin1, a known protein partner of Snap25, as a positive control of in vivo coimmunoprecipitation.

In Vitro Degradation Experiments of Truncated PRRT2

To generate the remaining three N-terminal HA-tagged PRRT2 truncation mutation constructs (HA-R240X, HA-E173X, and HA-I327Ifs*14), site-directed mutagenesis was performed with the QuikchangeII Site-Directed Mutagenesis Kit described above. HEK293T cells were cotransfected with equal amounts of WT FLAG-PRRT2 construct and either WT HA-PRRT2 or one of the four truncation mutations with the FuGene HD transfection reagent. HEK293T cells were grown, harvested 36 hr after transfection, then homogenized in 1 ml of RIPA buffer with protease and phosphatase inhibitors. Western blotting was performed as described above. A rabbit anti-HA antibody was used for detecting HA-tagged PRRT2, and a mouse anti-FLAG antibody was used for detecting FLAG-tagged PRRT2. A mouse anti-GAPDH antibody (1:5000, Millipore) was also applied on blots as a loading control.

Primary Neuronal Culture and Immunofluorescence Microscopy

Hippocampal neurons were isolated from day 20 rat embryos in accordance with UCSF IACUC guidelines, transfected with plasmids containing FLAG-tagged WT and mutant human PRRT2 by electroporation (Amaxa), and cultured as previously described (Li et al., 2005). Fixed cells were immunostained with mouse anti-FLAG M2 monoclonal antibody (Sigma) and rabbit anti-Synapsin (Abcam) or mouse anti-MAP2 (Sigma) antibodies at a dilution of 1:500. Alexa488, Alexa 546 (Invitrogen), and Dylite 549-conjugated secondary antibodies (Jackson ImmunoResearch) were used at a dilution of 1:500. Images were obtained with a Zeiss LSM 510 Meta confocal microscope.

ACCESSION NUMBERS

The GenBank accession number for the PRRT2 sequence reported in this paper is BC011405.

SUPPLEMENTAL INFORMATION

Supplemental Information includes seven figures and three tables and can be found with this article online at doi:10.1016/j.celrep.2011.11.001.

LICENSING INFORMATION

ACKNOWLEDGMENTS

We thank Dr. Nicholas Lenn for patient referrals. We are grateful to all the families for their participation in this research. This work was supported by grants from the Dystonia Medical Research Foundation, the Bachmann-Strauss Dystonia Parkinson Foundation, NIH (grant NS043533 to L.P., grant U54 RR19481), the Sandler Neurogenetics Fund (Y.-H.F. and L.P.), ANR (grant EPILAND to P.S.), and INSERM. L.J.P. is an investigator of the Howard Hughes Medical Institute.

Received: September 19, 2011
Revised: October 21, 2011
Accepted: November 7, 2011
Published online: December 15, 2011

WEB RESOURCES

The URLs for data presented herein are as follows:

1000 Genomes, http://www.1000genomes.org/
cgatools, cgatools.sourceforge.net
CGI, http://www.completegenomics.com
CGI public genomes, ftp://ftp2.completegenomics.com/
Circos, http://circos.ca
ClustalW2, http://www.ebi.ac.uk/Tools/msa/clustalw2/
dbSNP, http://www.ncbi.nlm.nih.gov/projects/SNP/
Ensembl: http://uswest.ensembl.org/index.html
HapMap, http://www.hapmap.org
NCBI, http://www.ncbi.nlm.nih.gov/
UCSC Genome Bioinformatics, http://genome.ucsc.edu/
TMHMM Server, http://www.cbs.dtu.dk/services/TMHMM/
TMpred - Prediction of Transmembrane Regions and Orientation, http://www.ch.embnet.org/software/TMPRED_form.html

REFERENCES

Abe, T., Kobayashi, M., Araki, K., Kodama, H., Fujita, Y., Shinozaki, T., and Ushijima, H. (2000). Infantile convulsions with mild gastroenteritis. Brain Dev. *22*, 301–306.

Bennett, L.B., Roach, E.S., and Bowcock, A.M. (2000). A locus for paroxysmal kinesigenic dyskinesia maps to human chromosome 16. Neurology *54*, 125–130.

Bhatia, K.P. (2011). Paroxysmal dyskinesias. Mov. Disord. *26*, 1157–1165.

Blakeley, J., and Jankovic, J. (2002). Secondary paroxysmal dyskinesias. Mov. Disord. *17*, 726–734.

Bruno, M.K., Hallett, M., Gwinn-Hardy, K., Sorensen, B., Considine, E., Tucker, S., Lynch, D.R., Mathews, K.D., Swoboda, K.J., Harris, J., et al. (2004). Clinical evaluation of idiopathic paroxysmal kinesigenic dyskinesia: new diagnostic criteria. Neurology *63*, 2280–2287.

Bruno, M.K., Lee, H.Y., Auburger, G.W., Friedman, A., Nielsen, J.E., Lang, A.E., Bertini, E., Van Bogaert, P., Averyanov, Y., Hallett, M., et al. (2007). Genotype-phenotype correlation of paroxysmal nonkinesigenic dyskinesia. Neurology *68*, 1782–1789.

Callenbach, P.M., van den Boogerd, E.H., de Coo, R.F., ten Houten, R., Oosterwijk, J.C., Hageman, G., Frants, R.R., Brouwer, O.F., and van den

Maagdenberg, A.M. (2005). Refinement of the chromosome 16 locus for benign familial infantile convulsions. Clin. Genet. *67*, 517–525.

Camac, A., Greene, P., and Khandji, A. (1990). Paroxysmal kinesigenic dystonic choreoathetosis associated with a thalamic infarct. Mov. Disord. *5*, 235–238.

Caraballo, R., Pavek, S., Lemainque, A., Gastaldi, M., Echenne, B., Motte, J., Genton, P., Cersósimo, R., Humbertclaude, V., Fejerman, N., et al. (2001). Linkage of benign familial infantile convulsions to chromosome 16p12-q12 suggests allelism to the infantile convulsions and choreoathetosis syndrome. Am. J. Hum. Genet. *68*, 788–794.

Clark, J.D., Pahwa, R., Koller, C., and Morales, D. (1995). Diabetes mellitus presenting as paroxysmal kinesigenic dystonic choreoathetosis. Mov. Disord. *10*, 353–355.

Demirkiran, M., and Jankovic, J. (1995). Paroxysmal dyskinesias: clinical features and classification. Ann. Neurol. *38*, 571–579.

Drake, M.E., Jr. (1987). Paroxysmal kinesigenic choreoathetosis in hyperthyroidism. Postgrad. Med. J. *63*, 1089–1090.

Drmanac, R., Sparks, A.B., Callow, M.J., Halpern, A.L., Burns, N.L., Kermani, B.G., Carnevali, P., Nazarenko, I., Nilsen, G.B., Yeung, G., et al. (2010). Human genome sequencing using unchained base reads on self-assembling DNA nanoarrays. Science *327*, 78–81.

Du, T., Feng, B., Wang, X., Mao, W., Zhu, X., Li, L., Sun, B., Niu, N., Liu, Y., Wang, Y., et al. (2008). Localization and mutation detection for paroxysmal kinesigenic choreoathetosis. J. Mol. Neurosci. *34*, 101–107.

Harbour, J.W., Onken, M.D., Roberson, E.D., Duan, S., Cao, L., Worley, L.A., Council, M.L., Matatall, K.A., Helms, C., and Bowcock, A.M. (2010). Frequent mutation of BAP1 in metastasizing uveal melanomas. Science *330*, 1410–1413.

Hattori, H., and Yorifuji, T. (2000). Infantile convulsions and paroxysmal kinesigenic choreoathetosis in a patient with idiopathic hypoparathyroidism. Brain Dev. *22*, 449–450.

Hu, K., Carroll, J., Fedorovich, S., Rickman, C., Sukhodub, A., and Davletov, B. (2002). Vesicular restriction of synaptobrevin suggests a role for calcium in membrane fusion. Nature *415*, 646–650.

Huang, Y.G., Chen, Y.C., Du, F., Li, R., Xu, G.L., Jiang, W., and Huang, J. (2005). Topiramate therapy for paroxysmal kinesigenic choreoathetosis. Mov. Disord. *20*, 75–77.

Kikuchi, T., Nomura, M., Tomita, H., Harada, N., Kanai, K., Konishi, T., Yasuda, A., Matsuura, M., Kato, N., Yoshiura, K., and Niikawa, N. (2007). Paroxysmal kinesigenic choreoathetosis (PKC): confirmation of linkage to 16p11-q21, but unsuccessful detection of mutations among 157 genes at the PKC-critical region in seven PKC families. J. Hum. Genet. *52*, 334–341.

Lee, W.L., Tay, A., Ong, H.T., Goh, L.M., Monaco, A.P., and Szepetowski, P. (1998). Association of infantile convulsions with paroxysmal dyskinesias (ICCA syndrome): confirmation of linkage to human chromosome 16p12-q12 in a Chinese family. Hum. Genet. *103*, 608–612.

Lee, H.Y., Xu, Y., Huang, Y., Ahn, A.H., Auburger, G.W., Pandolfo, M., Kwiecinski, H., Grimes, D.A., Lang, A.E., Nielsen, J.E., et al. (2004). The gene for paroxysmal non-kinesigenic dyskinesia encodes an enzyme in a stress response pathway. Hum. Mol. Genet. *13*, 3161–3170.

Lee, H.Y., Nakayama, J., Xu, Y., Fan, X., Karouani, M., Shen, Y., Pothos, E.N., Hess, E.J., Fu, Y.H., Edwards, R.H., and Ptáček, L.J. (2012). Dopamine dysregulation in a mouse model of paroxysmal non-kinesigenic dyskinesia. J. Clin. Invest. Published online January 3, 2012.

Li, H., Waites, C.L., Staal, R.G., Dobryy, Y., Park, J., Sulzer, D.L., and Edwards, R.H. (2005). Sorting of vesicular monoamine transporter 2 to the regulated secretory pathway confers the somatodendritic exocytosis of monoamines. Neuron *48*, 619–633.

Lipton, J., and Rivkin, M.J. (2009). 16p11.2-related paroxysmal kinesigenic dyskinesia and dopa-responsive parkinsonism in a child. Neurology *73*, 479–480.

Mirsattari, S.M., Berry, M.E., Holden, J.K., Ni, W., Nath, A., and Power, C. (1999). Paroxysmal dyskinesias in patients with HIV infection. Neurology *52*, 109–114.

Müller, U. (2009). The monogenic primary dystonias. Brain *132*, 2005–2025.

Ono, S., Yoshiura, K., Kurotaki, N., Kikuchi, T., Niikawa, N., and Kinoshita, A. (2011). Mutation and copy number analysis in paroxysmal kinesigenic dyskinesia families. Mov. Disord. *26*, 761–763.

Robinson, J.T., Thorvaldsdóttir, H., Winckler, W., Guttman, M., Lander, E.S., Getz, G., and Mesirov, J.P. (2011). Integrative genomics viewer. Nat. Biotechnol. *29*, 24–26.

Rochette, J., Roll, P., and Szepetowski, P. (2008). Genetics of infantile seizures with paroxysmal dyskinesia: the infantile convulsions and choreoathetosis (ICCA) and ICCA-related syndromes. J. Med. Genet. *45*, 773–779.

Roll, P., Sanlaville, D., Cillario, J., Labalme, A., Bruneau, N., Massacrier, A., Délepine, M., Dessen, P., Lazar, V., Robaglia-Schlupp, A., et al. (2010). Infantile convulsions with paroxysmal dyskinesia (ICCA syndrome) and copy number variation at human chromosome 16p11. PLoS ONE *5*, e13750.

Ryan, D.P., and Ptácek, L.J. (2010). Episodic neurological channelopathies. Neuron *68*, 282–292.

Schneider, S.A., Paisan-Ruiz, C., Garcia-Gorostiaga, I., Quinn, N.P., Weber, Y.G., Lerche, H., Hardy, J., and Bhatia, K.P. (2009). GLUT1 gene mutations cause sporadic paroxysmal exercise-induced dyskinesias. Mov. Disord. *24*, 1684–1688.

Sørensen, J.B., Matti, U., Wei, S.H., Nehring, R.B., Voets, T., Ashery, U., Binz, T., Neher, E., and Rettig, J. (2002). The SNARE protein SNAP-25 is linked to fast calcium triggering of exocytosis. Proc. Natl. Acad. Sci. USA *99*, 1627–1632.

Stelzl, U., Worm, U., Lalowski, M., Haenig, C., Brembeck, F.H., Goehler, H., Stroedicke, M., Zenkner, M., Schoenherr, A., Koeppen, S., et al. (2005). A human protein-protein interaction network: a resource for annotating the proteome. Cell *122*, 957–968.

Suls, A., Dedeken, P., Goffin, K., Van Esch, H., Dupont, P., Cassiman, D., Kempfle, J., Wuttke, T.V., Weber, Y., Lerche, H., et al. (2008). Paroxysmal exercise-induced dyskinesia and epilepsy is due to mutations in SLC2A1, encoding the glucose transporter GLUT1. Brain *131*, 1831–1844.

Swoboda, K.J., Soong, B., McKenna, C., Brunt, E.R., Litt, M., Bale, J.F., Jr., Ashizawa, T., Bennett, L.B., Bowcock, A.M., Roach, E.S., et al. (2000). Paroxysmal kinesigenic dyskinesia and infantile convulsions: clinical and linkage studies. Neurology *55*, 224–230.

Szepetowski, P., Rochette, J., Berquin, P., Piussan, C., Lathrop, G.M., and Monaco, A.P. (1997). Familial infantile convulsions and paroxysmal choreoathetosis: a new neurological syndrome linked to the pericentromeric region of human chromosome 16. Am. J. Hum. Genet. *61*, 889–898.

Tarsy, D., and Simon, D.K. (2006). Dystonia. N. Engl. J. Med. *355*, 818–829.

Thiriaux, A., de St Martin, A., Vercueil, L., Battaglia, F., Armspach, J.P., Hirsch, E., Marescaux, C., and Namer, I.J. (2002). Co-occurrence of infantile epileptic seizures and childhood paroxysmal choreoathetosis in one family: clinical, EEG, and SPECT characterization of episodic events. Mov. Disord. *17*, 98–104.

Tomita, H., Nagamitsu, S., Wakui, K., Fukushima, Y., Yamada, K., Sadamatsu, M., Masui, A., Konishi, T., Matsuishi, T., Aihara, M., et al. (1999). Paroxysmal kinesigenic choreoathetosis locus maps to chromosome 16p11.2-q12.1. Am. J. Hum. Genet. *65*, 1688–1697.

Weber, Y.G., Berger, A., Bebek, N., Maier, S., Karafyllakes, S., Meyer, N., Fukuyama, Y., Halbach, A., Hikel, C., Kurlemann, G., et al. (2004). Benign familial infantile convulsions: linkage to chromosome 16p12-q12 in 14 families. Epilepsia *45*, 601–609.

Weber, Y.G., Storch, A., Wuttke, T.V., Brockmann, K., Kempfle, J., Maljevic, S., Margari, L., Kamm, C., Schneider, S.A., Huber, S.M., et al. (2008). GLUT1 mutations are a cause of paroxysmal exertion-induced dyskinesias and induce hemolytic anemia by a cation leak. J. Clin. Invest. *118*, 2157–2168.

Zhao, N., Hashida, H., Takahashi, N., and Sakaki, Y. (1994). Cloning and sequence analysis of the human SNAP25 cDNA. Gene *145*, 313–314.

Zittel, S., Bester, M., Gerloff, C., Munchau, A., and Leypoldt, F. (2011). Symptomatic paroxysmal kinesigenic choreoathetosis as primary manifestation of multiple sclerosis. J. Neurol. Published online July 30, 2011.